nature biotechnology

Fluorescent peptides highlight peripheral nerves during surgery in mice

Michael A Whitney[1], Jessica L Crisp[2], Linda T Nguyen[3], Beth Friedman[1], Larry A Gross[4], Paul Steinbach[4], Roger Y Tsien[1,2,4] & Quyen T Nguyen[3]

Nerve preservation is an important goal during surgery because accidental transection or injury leads to significant morbidity, including numbness, pain, weakness or paralysis. Nerves are usually identified by their appearance and relationship to nearby structures or detected by local electrical stimulation (electromyography), but thin or buried nerves are sometimes overlooked. Here, we use phage display to select a peptide that binds preferentially to nerves. After systemic injection of a fluorescently labeled version of the peptide in mice, all peripheral nerves are clearly delineated within 2 h. Contrast between nerve and adjacent tissue is up to tenfold, and useful contrast lasts up to 8 h. No changes in behavior or activity are observed after treatment, indicating a lack of obvious toxicity. The fluorescent probe also labels nerves in human tissue samples. Fluorescence highlighting is independent of axonal integrity, suggesting that the probe could facilitate surgical repair of injured nerves and help prevent accidental transection.

Accidental transection or injury of nerves during surgery can lead to significant patient morbidity including chronic pain or permanent paralysis. Thin or buried nerves are particularly difficult to distinguish and are therefore the most likely to be damaged during surgical procedures.

Identification of motor nerves before direct exposure is currently dependent on electromyographic (EMG) monitoring[1–3], in which a stimulating electrode is inserted and distal muscle twitches are monitored. EMG is not an imaging technique, so even if a nerve has been identified in one location, there is no visual guidance for how far from the stimulation site the nerve lies. Furthermore, EMG identifies only motor pathways, not sensory fibers such as the first two divisions of the trigeminal nerves, the cochleovestibular nerve or the neurovascular bundle surrounding the prostate gland[4,5], where nerve injury during radical prostatectomy leads to significant urinary incontinence and erectile dysfunction[6]. Finally, EMG fails if axonal or neuromuscular transmission is temporarily blocked distal to the recording site by nerve compression, trauma, tumor invasion, local anesthetics or neuromuscular blockers. Although there are developing technologies for *in vivo* nerve visualization such as optical coherence tomography[7] or laser confocal microscopy[8], these technique have focused on the visualization of the optic or other superficial nerves and may not be generally applicable for viewing nerves in a surgical setting.

Current methods for nerve labeling during surgery depend on retrograde or anterograde tracing of individual axonal tracts using fluorescent dyes[9–12]. The dyes are applied either to the innervation target and travel in a retrograde fashion to label the innervating nerve fibers or directly to identified nerves and label nerve fibers in both anterograde and retrograde directions. Local injections have the drawback of only labeling one nerve fiber tract at a time and that axonal labeling is limited. Axonal transport is relatively slow and it can take days to label a single human nerve. Furthermore, the direct injection of fluorescent dyes contaminates the surgical site with excess fluorescent dyes and may be damaging to the target organs or nerve of interest.

In this study, we describe the development of peptides by phage display[13] that preferentially bind to peripheral nerve tissue compared to adjacent non-nerve tissue after systemic administration.

We used *in vitro* selection with either excised murine peripheral nerves or purified myelin basic protein (MBP) and *in vivo* selection where phage were injected into living mice and nerves were harvested for phage isolation. From the *in vitro* selection against MBP, a single phage with its variable sequence coding for the peptide TYTDWLNFWAWP (NP39) was identified (**Supplementary Fig. 1**).

The *in vitro* selection against excised peripheral nerves yielded three sequences that were repeatedly observed. Of 14 specific phage sequences at the end of seven rounds of selection, 5 coded for NTQTLAKAPEHT (NP41), 3 for KSLSRHDHIHHH (NP40) and 2 for DFTKTSPLGIH (NP42). The remaining phage sequences were each represented only once (**Supplementary Fig. 1**). The *in vivo* selection did not yield any duplicated phage after eight rounds of selection, perhaps because vigorous washing to remove mechanically entangled or loosely bound phage is not possible in a live animal. One sequence selected *in vivo*, AHHNSWKAKHHS (NP38), was chosen for further testing because it contained multiple histidines reminiscent of NP40. Both NP40 and NP38 have been previously identified in various phage selection schemes for binding to proteins (scFV, GST-FLAS-DRD) or hepatoma cell lines, which could indicate that these peptides either bind nonspecifically to proteins or cells or alternatively that they bind to substrates common to both screens[14–17].

[1]Department of Pharmacology, University of California at San Diego, La Jolla, California, USA. [2]Department of Chemistry and Biochemistry, University of California at San Diego, La Jolla, California, USA. [3]Division of Otolaryngology-Head and Neck Surgery, University of California at San Diego, La Jolla, California, USA. [4]Howard Hughes Medical Institute, University of California at San Diego, La Jolla, California, USA. Correspondence should be addressed to Q.T.N. (quyennguyen@ucsd.edu).

Received 3 August 2010; accepted 4 January 2011; published online 6 February 2011; doi:10.1038/nbt.1764

Figure 1 Whole-body survey of nerves in mice ($n = 3$) 4 h after injection with 450 nmoles of FAM-NP41. (**a**,**b**) Brachial plexus. Reflectance image (**a**) showing left brachial plexus (arrow). Smaller branches (~50–100 µm) are easily seen (arrowheads) with fluorescence labeling (**b**) but not in reflectance image. (**c**,**d**) Sciatic nerve. Reflectance image (**c**) showing right sciatic nerve (arrow). Many more small branches (~50–100 µm) are seen (arrowheads) with fluorescence imaging (**b**) compared to reflectance. (**e**,**f**) Phrenic nerve. Reflectance image (**e**) showing left phrenic nerve (arrow) descending from the mediastinum to innervate the diaphragm. Note that the nerve is seen as a single linear fluorescent structure (arrow, **f**) compared to the bundle of nerve and connective tissue seen with reflectance (arrow, **e**). Arrowhead points to an intercostal nerve which is easily seen with fluorescence but not with reflectance. (**g**,**h**) Dorsal cutaneous nerves. Reflectance image (**g**) showing the dorsal musculature. Fluorescence imaging highlights the dorsal intercostal nerves (arrows, **h**) that are not easily seen with reflectance. (**i**,**j**) Facial nerve**.** Main facial nerve branches (arrows) are easily seen with both reflectance (**i**) and fluorescence (**j**). However, a small branch of nerve arborization (arrowhead) leading to the upper face can be distinguished from surrounding tissue with fluorescence but not with reflectance. Insert shows arborizations (~50 µm diameter) of the lower division of the facial nerve that can be easily seen with fluorescence labeling. (**k**,**l**) Dorsal view of skull base. Reflectance image (**k**) showing left facial nerve (large arrow) wrapping around the ear, trigeminal nerves (small arrows), optic nerves (large arrowhead) and optic chiasm (small arrowhead). Fluorescence image (**l**) shows fluorescence labeling of the facial and trigeminal nerves (peripheral nervous system) but not the optic nerves and chiasm (central nervous system). Scale bar (**a**–**l**), 5 mm; inserts (**i** and **j**), 1 mm.

Sequences NP38, 40, 41, 42 and a control peptide containing the shared amino acids in random order were similarly synthesized as fluorescein-5(6)-carbonyl group (FAM) conjugates on a C-terminal lysinamide. To test nerve binding affinity *in vivo* of each of the identified sequences, we injected FAM-labeled peptides intravenously into living mice and evaluated the contrast between nerve and muscle 2–4 h after injection. The sequence identified through *in vitro* selection against MBP (NP39) and the sequence identified through the *in vivo* selection (NP38) did not have significant nerve-to-muscle contrast and both showed high-background binding to the surrounding nonneural tissue. The peptide sequence identified most often in *in vitro* selection against excised nerves NP41 had the best nerve to nonnerve contrast. The other two sequences, NP40 and NP42, identified through this same selection strategy also yielded some nerve-to-muscle contrast, although less than that of NP41 (**Supplementary Table 1**). A systemic survey of animals injected with FAM-NP41 revealed that all peripheral nerves and their arborizations (including nerve branches as small as 50 µmin diameter) were brightly labeled, including motor pathways, and sensory nerves such as the first two divisions of the trigeminal nerves (**Fig. 1**). The central nervous system did not appear to take up any fluorescence, perhaps because the peptide did not cross the blood-brain barrier.

To evaluate the kinetics of peptide nerve binding *in vivo*, we imaged sciatic nerves and surrounding nonnerve tissue in mice before and after intravenous administration of FAM-NP41. Before administration of the peptide, there was little contrast between the nerve (small yellow arrowheads) and surrounding nonnerve tissue (**Supplementary Fig. 2a**). Within seconds after intravenous administration of FAM-NP41, fluorescence could be seen leaking from capillaries (arrows) associated with the sciatic nerves (insert, **Supplementary Fig. 2b**). Nerve fluorescence peaked at 10 min after administration (**Supplementary Fig. 2c**) and declined thereafter to a plateau (**Fig. 2a**). Muscle fluorescence was highest immediately after intravenous administration of the peptide, with a half-life of ~20 min ($n = 5$, **Fig. 2a**). Serum half-life was calculated at ~10 min ($n = 5$, **Fig. 2b**). Useful contrast between nerve and surrounding tissue developed by 2 h after injection ($n = 5$, **Fig. 2c** and **Supplementary Fig. 2e**) and lasted several hours (**Fig. 2a**,**c** and **Supplementary Fig. 2e**,**f**), reaching seven- to tenfold by 4–5 h ($n = 5$, **Fig. 2c**). By 24 h after injection, all visible staining had disappeared ($n = 20$). Intravenous injection of the mirror-image peptide with all D-amino acids showed nerve staining at the level of carboxyfluorescein alone (**Supplementary Fig. 3**). The nerve-to-surrounding tissue contrast ratio was correlated with the amount of peptide administered over the range of 15 to 5,000 nmoles per mouse (**Fig. 2d**).

We attempted topical application of FAM-NP41 to label mouse sciatic nerves *in vivo*, however, incomplete wash-out of probe and residual fluorescence due to the probe infiltrating into tissue pockets led to the appearance of linear structures that could be mistaken for nerve fibers.

To evaluate the localization of NP41 binding within nerves, we injected peptide into thy1-YFP transgenic mice whose axons were genetically encoded with YFP under a neuron-specific promoter[18]. To avoid spectral overlap with YFP and to allow imaging deeper in tissues, we replaced FAM with the deep red fluorophore Cy5. Cy5-NP41 precisely labeled nerves that expressed YFP and correlated with nerve fibers as seen in brightfield imaging (**Fig. 3a**–**c**). No nerve-to-muscle contrast was detected in mice injected with unconjugated Cy5 (**Supplementary Fig. 4a**).

To confirm that changing the fluorophore does not change nerve distribution of NP41, we imaged frozen cross-sections of nerves from mice that had been injected with either 150 nmols FAM-NP41 or Cy5-NP41. Imaged cross-sections showed that labeling was comparable using the two fluorophores (**Supplementary Fig. 4b**,**c**). To determine if the NP41 was labeling axons, we imaged 3–5 µm cryosections of nerves from thy1-YFP animals treated with Cy5-NP41. Cy5-NP41 localized to the epineurium of the nerves with some labeling of the perineurium and endoneurium, but did not colocalize with either myelin or axons (**Fig. 3d**–**i**).

To evaluate the ability of NP41 to highlight nerve branches that were buried within tissue, we compared visibility of standard white light reflectance and fluorescent images of Cy5-NP41 and YFP-labeled axons.

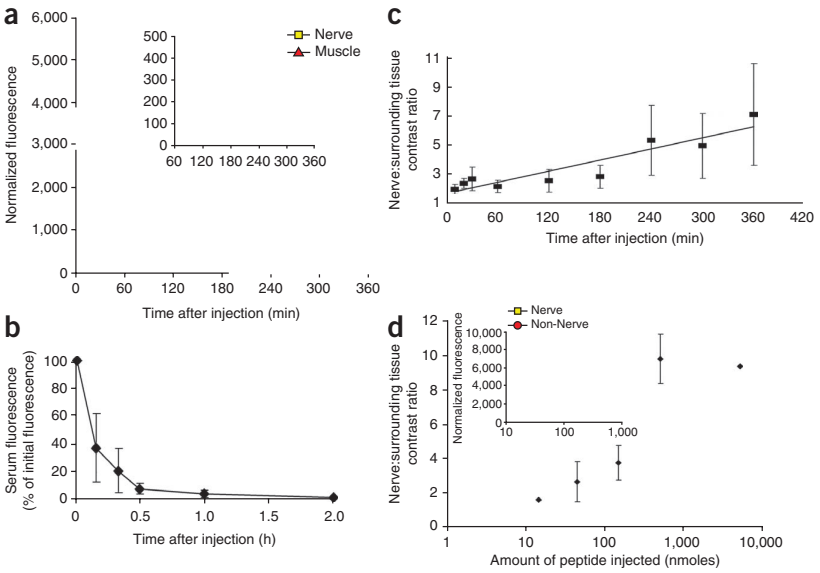

Figure 2 Time course and dose response of FAM-NP41 binding to nerve and nonnerve tissue. (**a**–**d**) Nerve fluorescence peaked at around 10 min after administration (**a**), then declined (half-life ~50 min) to a plateau sustained between 3 and 6 h (see inset with expanded intensity scale, Student's *t*-test, two–tailed, $P = 0.002$ at 2 h, 0.0007 at 3 h, 0.0007 at 4 h, 0.003 at 5 h, 0.006 at 6 h). In contrast, muscle fluorescence was highest immediately after intravenous administration of the peptide, then declined steadily with a half-life of ~20 min (**a**). Serum half-life was calculated at ~10 min (**b**). Useful contrast between nerve and surrounding muscle developed by 2 h and lasts several hours (**c**). Nerve-to–surrounding tissue contrast ratio increased with increasing amount of peptide injected, concentration from 15 to 5,000 nmoles per mouse injected ($n = 2$) (**d**), because surrounding nonnerve tissue fluorescence seems more saturable than nerve binding with increasing peptide concentration (inset).

Cy5-NP41 (**Fig. 3c**, insert arrows) was better than brightfield (**Fig. 3a**, insert) or YFP (**Fig. 3b**, insert) at highlighting nerves that were branching deep into muscle. Nerve branches not on the surface were essentially invisible with reflectance imaging (long arrow, arrowheads, **Fig. 4a**). However, these buried branches can be visualized with Cy5-NP41 (arrowheads and long arrow, **Fig. 4b**) and YFP (arrowheads, **Fig. 4c**).

We also assessed the visibility of nerve branches covered by breast cancer tumor in syngeneic graft models[19,20]. For this evaluation we co-administered Cy5-labeled dendrimer conjugates of activatable, cell-penetrating peptides (ACPPs), which highlight tumor margins and FAM-NP41 (refs. 19,20). As shown, nerve branches that descend into the tumor become invisible with reflectance imaging (arrowhead, **Fig. 4d**); however, these buried branches could be visualized, with FAM-NP41 (arrowhead, **Fig. 4e**) protruding into the tumor which has been labeled with Cy5 dendrimer (**Fig. 4f**). The ACPP marks the tumor to be excised, whereas the NP41 highlights the nerve tissue whose preservation is most essential.

Mice showed no change in behavior or activity after injections of 15–5,000 nmoles of FAM-NP41 or 75–300 nmoles Cy5-NP41. In addition, mice that had been injected with 15 nmoles ($n = 2$), 45 nmoles ($n = 2$), 150 nmoles ($n = 2$), 450 nmoles ($n = 2$), 5,000 nmoles ($n = 1$) showed no significant weight changes or morbidity through 8 weeks of monitoring compared to uninjected mice ($n = 2$). In addition, injection of 150 nmoles of FAM-NP41 had no effect on the shape, amplitude or latency of compound muscle action potential[21] (**Supplementary Fig. 5**), indicating NP41 has no acute effect on peripheral nerve conduction or neuromuscular transmission.

To evaluate the biodistribution of the peptide after systemic administration, organs were harvested from mice intravenously injected with 150 nmoles FAM-NP41 or Cy5-NP41 and fluorescence uptake was evaluated. The majority of the fluorescence accumulated in the kidney and was excreted into the urine. Liquid chromatography–electrospray mass spectrometry of the urine gave different peaks from normal mouse urine spiked with intact FAM-NP41 or Cy5-NP41, indicating that the injected peptides had been efficiently metabolized. The major fluorescently labeled species identified by matrix-assisted laser desorption/ionization mass spectrometry were cysteinamide-Cy5

Figure 3 Cy5-NP41 (acetyl-SHSNTQTLAKAPEHTGC-(Cy5)-amide) labeling of sciatic nerve in Thy1-YFP transgenic mice. (**a**) Low-power brightfield view of left exposed sciatic nerve. Inset shows magnified view of central boxed region. (**b**) Same nerve as in **a** with YFP fluorescence (pseudocolored yellow) superimposed on the brightfield image, showing transgenic expression of YFP in axons. (**c**) Same nerve as in **a** and **b** viewed with Cy5 fluorescence (pseudocolored cyan for maximal contrast during live surgery) superimposed on the brightfield image, showing nerve labeling with Cy5-NP41. Arrows in **b** and **c** point to thin buried nerve branches that are better revealed by the long-wavelength Cy5 fluorescence than by brightfield reflectance or shorter-wavelength YFP fluorescence. There is some nonspecific labeling of skin (asterisk) and cut edges of muscle (arrowhead) by Cy5-NP41. Fortunately, such nonspecific labeling hardly ever has the filamentous appearance of nerves, so an experienced surgeon can usually distinguish nonspecific from specific targets. (**d**) Low magnification longitudinal section showing myelin within the sciatic nerve using differential interference contrast (DIC), pseudocolored blue. (**e**) Same nerve as in **d** showing axoplasmic YFP pseudocolored green (arrows). (**f**) Same nerve as in **d** and **e**, showing Cy5-NP41 labeling (pseudocolored red) of epineurium (arrows) and endoneurium (arrowheads). (**g**) Composite image of **d**, **e** and **f** showing that NP41 labeling does not colocalize with either myelin or axoplasm. (**h**–**k**) Cross-sectional images corresponding to panels **e**–**g**.

Figure 4 NP41 can highlight buried nerve branches invisible by standard illumination. (**a**–**c**) Right facial nerve and its arborizations in a thy1-YFP mouse treated with Cy5-NP41, viewed by (**a**) white light reflectance, (**b**) Cy5 fluorescence (pseudocolored cyan) overlaid on reflectance and (**c**) YFP fluorescence (pseudocolored yellow), also overlaid on reflectance. The short arrow marks a nerve branch visible by all three imaging modes. The arrowheads point to branches that are difficult to differentiate from muscle fascia in reflectance, but clearly distinguishable in both fluorescence images. The long arrow indicates a deeply buried branch visible only by Cy5-NP41 due to the better penetration of far-red wavelengths. (**d**–**f**) Left sciatic nerve (arrow) and its arborization in a mouse with a syngeneic 8119 mammary tumor graft[17,18], viewed by (**d**) white light reflectance, (**e**) FAM fluorescence 2 h after intravenous injection of NP41 (150 nmoles) (pseudocolored cyan, overlaid on reflectance) and (**f**) Cy5 fluorescence (pseudocolored green, overlaid on reflectance) from conjugates of activatable cell-penetrating peptides and dendrimers (ACPPDs). The large arrowheads in **d** and **e** point to a nerve branch buried under tumor, visible only by FAM fluorescence. Small arrowheads in **f** denote tumor. See **Supplementary Video 1**.

and lysinamide-FAM from mice injected with Cy5-NP41 or FAM-NP41, respectively. Small fractions of successive fragments of NP41 starting from the C terminus were also recovered, suggesting that the entire peptide had been sequentially degraded from the N terminus (**Supplementary Fig. 6c**,**d**). In contrast, in urine from mice injected with control all D-amino acid FAM-NP41, the full-length peptide was recovered intact (**Supplementary Fig. 6e**).

In addition to labeling healthy nerves during nontrauma related surgery, the ability to label and identify severed or injured nerves is also of considerable clinical utility. Such, visualization of injured or severed nerves could guide procedures such as rejoining severed nerves leading to better prognosis after injury. In the cases of injury involving motor nerves, EMG may fail because severed nerves typically lack functionality. Direct labeling could also prove useful when EMG detection does not work because swelling or inflammation leads to short-term loss of nerve conduction. Nerve labeling by FAM-NP41 was 100% of contralateral intact nerve immediately and 1 d after crush injury, decreased by 40% at day 3 and was back to 100% 7 d after injury (**Supplementary Fig. 7a**–**f**,**i**). Because we detected a transient decrease in uptake upon crush injury, we tested if this effect could potentially be due to a temporary decrease in blood flow to the nerve tissue thereby inhibiting uptake. As predicted, nerve devascularization (by intentional injury to the feeding vessels before peptide administration) greatly diminished subsequent uptake of FAM-NP41 (**Supplementary Fig. 7g**,**h**).

To evaluate whether NP41 could highlight human as well as mouse nerves, freshly resected recurrent laryngeal nerves and adjacent muscle obtained from patients undergoing total laryngectomy were incubated with FAM-NP41. Selective binding of FAM-NP41 to nerves as compared to adjacent muscle was observed (**Supplementary Fig. 8a**,**b**). Histological examination of tissue sections showed that the fluorescence was concentrated in the connective tissue surrounding the nerve, that is, epineurium, perineurium and endoneurium (**Supplementary Fig. 8c**–**h**), similar to the binding pattern in murine nerves. Although we cannot administer NP41 to human subjects without much further testing and regulatory approval, these *ex vivo* tests provide preliminary evidence that NP41 could cross-react with human nerves.

The method of systemic injection of fluorescently labeled peptides to label nerves overcomes some of the major disadvantages of currently available fluorescent tracers, which provide only localized labeling, have low signal-to-noise ratio and require preoperative lead time incompatible with most surgical procedures.

Our peptide localizes predominantly to nerve-associated connective tissue and not to myelin or axonal membranes, which may explain why there were no pharmacological or toxic effects observed in our preliminary toxicity assessments. We achieve good contrast of all nerves in the body including motor and sensory nerves within 2–3 h compared to tracers that have to be transported in an anterograde or retrograde direction and can require days to label. Contrast from our systemically injected peptides lasts several hours, which would be long enough for most typical operations. A probe of this sort could potentially be further optimized to minimize wash-out time allowing the agents to be provided intravenously within minutes before skin incision. We believe that eventually the use of fluorescently labeled probes for nerve visualization will be routine and will decrease the incidence of inadvertent injury during surgery and may improve identification and repair of nerves after trauma thereby leading to improved patient prognosis.

We were able to detect nerve arborizations as small as 50 μm, which is at least one order of magnitude smaller than most surgically relevant nerves in the human body. In addition, the peptide is cleared within 24 h and completely metabolized, which should reduce the chance of side effects. We would like to optimize NP41 and are therefore using a variety of methods to identify the molecular target(s) to which peptide NP41 binds. The identification of a specific target may allow setting up specific binding assays or using crystallographic information to determine structure-activity relationships and optimize NP41.

Even in the absence of a defined target, we can optimize for nerve affinity, decrease binding to negative tissues, shift fluorescence to longer wavelengths and modify pharmacology to improve contrast of NP41 or related molecules for improved *in vivo* imaging of nerves.

The minimal murine doses of NP41 used *in vivo* are currently equivalent to 1–3 g for a 70 kg person. This is within clinical dosing parameters for antibiotics, which are routinely given at such doses two to three times daily for systemic infections; intravenous immunoglobulins may be given in doses up to 150–300 g for a 70 kg person. As pharmacokinetic clearance is substantially slower in humans compared to mice, similar contrast may be achieved using a lower dose of NP41 or related contrast agent although slower pharmacokinetcs may increase lead time required before surgery. In addition to improving affinity/specificity of NP41 the attachments of macromolecular carriers or other controlled released formulation may be required to optimize this contrast agent for potential clinical use.

METHODS

Methods and any associated references are available in the online version of the paper at http://www.nature.com/naturebiotechnology/.

Note: Supplementary information is available on the Nature Biotechnology website.

ACKNOWLEDGMENTS

We are indebted to members of our laboratory for discussions and comments on the manuscript. Results described here are being used in support of a patent

filing by the University of California, San Diego. This work was supported by the Howard Hughes Medical Institute, grants from the Burrough-Wellcome Fund (Career Award for Medical Scientists) and National Institutes of Health (NIH, 5K08EB008122) to Q.T.N. and NIH grant NS27177 to R.Y.T.

AUTHOR CONTRIBUTIONS

M.A.W. designed and performed experiments, interpreted data and wrote manuscript. J.L.C. designed and performed experiments and interpreted data. L.T.N. designed and performed experiments and interpreted data. B.F. designed and performed experiments and interpreted data. L.A.G. designed and performed experiments and interpreted data. P.S. provided computer support for experiments, R.Y.T. designed experiments, interpreted data and wrote manuscript. Q.T.N. designed and performed experiments, interpreted data and wrote manuscript.

COMPETING FINANCIAL INTERESTS

The authors declare competing financial interests: details accompany the full-text HTML version of the paper at http://www.nature.com/naturebiotechnology/.

Published online at http://www.nature.com/naturebiotechnology/.
Reprints and permissions information is available online at http://npg.nature.com/reprintsandpermissions/.

1. Gantz, B.J. Intraoperative facial nerve monitoring. *Am. J. Otol.* Nov., (Suppl.), 58–61 (1985).
2. Davis, W.E., Rea, J.L. & Templer, J. Recurrent laryngeal nerve localization using a microlaryngeal electrode. *Otolaryngol. Head Neck Surg.* **87**, 330–333 (1979).
3. Miller, M.C. & Spiegel, J.R. Identification and monitoring of the recurrent laryngeal nerve during thyroidectomy. *Surg. Oncol. Clin. N. Am.* **17**, 121–144 (2008).
4. Walz, J., Graefen, M. & Huland, H. Basic principles of anatomy for optimal surgical treatment of prostate cancer. *World J. Urol.* **25**, 31–38 (2007).
5. Walz, J. *et al.* A critical analysis of the current knowledge of surgical anatomy related to optimization of cancer control and preservation of continence and erection in candidates for radical prostatectomy. *Eur. Urol.* **57**, 179–192 (2010).
6. Kübler, H.R. *et al.* Impact of nerve sparing technique on patient self-assessed outcomes after radical perineal prostatectomy. *J. Urol.* **178**, 488–492 (2007).
7. Zhivov, A., Blum, M., Guthoff, R. & Stachs, O. Real-time mapping of the subepithelial nerve plexus by in vivo confocal laser scanning microscopy. *Br. J. Ophthalmol.* **94**, 1133–1135 (2010).
8. Zysk, A.M., Nguyen, F.T., Oldenburg, A.L., Marks, D.L. & Boppart, S.A. Optical coherence tomography: a review of clinical development from bench to bedside. *J. Biomed. Opt.* **12**, 051403 (2007).
9. Kobbert, C. *et al.* Currents concepts in neuroanatomical tracing. *Prog. Neurobiol.* **62**, 327–351 (2000).
10. Richmond, F.J.R. *et al.* Efficacy of seven retrograde tracers, compared in multiple-labelling studies of feline motoneurones. *J. Neurosci. Methods* **53**, 35–46 (1994).
11. Marangos, N., Illing, R., Kruger, J. & Laszig, R. In vivo visualization of the cochlear nerve and nuclei with fluorescent axonal tracers. *Hear. Res.* **162**, 48–52 (2001).
12. O'Malley, M. *et al.* Fluorescent retrograde axonal tracing of the facial nerve. *Laryngoscope* **116**, 1792–1797 (2006).
13. Pasqualini, R. & Ruoslahti, E. Organ targeting in vivo using phage display peptide libraries. *Nature* **380**, 364–366 (1996).
14. Shtatland, T., Buettler, D., Kossodo, M., Pivovarov, M. & Weissleder, R. PepBank—a database of peptides based on sequence text mining and public peptide data sources. *BMC Bioinformatics* **8**, 280 (2007).
15. Berger, S., Bannantine, J.P. & Griffin, J.F.T. Autoreactive antibodies are present in sheep with Johne's disease and cross-react with *mycobacterium avium* subsp. *Paratuberculosis* antigens. *Microbes Infect.* **9**, 963–970 (2007).
16. Kim, G.S. *et al.* Suppression of receptor-mediated apoptosis by death effecter domain recruiting domain binding peptide aptamer. *Biochem. Biophys. Res. Commun.* **343**, 1165–1170 (2006).
17. Jiang, Y. *et al.* Targeting of hepatoma cell and suppression of tumor growth by a novel 12mer peptide fused to superantigen TSST-1. *Mol. Med.* **12**, 81–87 (2006).
18. Feng, G. *et al.* Imaging neuronal subsets in transgenic mice expressing multiple spectral variants of GFP. *Neuron* **28**, 41–51 (2000).
19. Olson, E.S. *et al.* Activatable cell penetrating peptides attached to nanoparticles: dual probes for fluorescence and magnetic resonance imaging of proteases in vivo. *Proc. Natl. Acad. Sci. USA* **107**, 4311–4316 (2010).
20. Nguyen, Q.T. *et al.* Surgery with molecular fluorescence imaging using activatable cell penetrating peptides decreases residual cancer and improves survival. *Proc. Natl. Acad. Sci. USA* **107**, 4317–4322 (2010).
21. Osuchowski, M.F., Teener, J. & Remick, D. Noninvasive model of sciatic nerve conduction in healthy and septic mice: reliability and normative data. *Muscle Nerve* **40**, 610–616 (2009).

ONLINE METHODS

All experiments on mice were performed under protocol approved by the University of California San Diego Institutional Animal Care and Use Committee.

Peptide selection with phage display. Phage display screens were used for *in vitro* selection of peptides binding to excised murine nerves or purified MBP and for an *in vivo* selection screen in which the phage library was injected in the tail vein of mice followed by dissection of nerve tissue and isolation of phage. For the *in vitro* selection, an m13 phage library expressing random 12-amino-acid sequences on the N terminus of gIII (New England Biolabs) were processed through two parallel *in vitro* selections for binding to either purified MBP or to excised murine nerves. In the selection against MBP, phage expressing a library of peptides were selected through multiple cycles for binding to biotinylated MBP, using avidin agarose to isolate selected phage. Specifically, the phage library was mixed with biotinylated MBP and allowed to bind for 1 h. Avidin agarose was added and incubated for an additional hour. Nonbinding phage were removed by washing the agarose three times with PBS solution and the supernatant was plated for titer and amplification for subsequent cycles. This process was repeated five times; once repeat sequences appeared, these were synthesized for affinity testing.

In the selection against excised murine nerves, phage from the same library as the selection against MBP were isolated based on differential binding to excised murine nerves and not to adjacent muscles and fat tissue. Phage were processed through multiple cycles of selection, with representative phage being isolated and sequenced after each cycle. Specifically, for positive selection using nerve tissue, nerve tissue was dissected/washed and mixed with a phage library. After incubation, the mixture (containing mostly intact nerves with phage particles that had variable affinity for nerves) was centrifuged and the pellet washed with PBS. The pellet was homogenized and plated for titering and reamplification. For negative selection using nonnerve tissues, nonnerve tissues (muscle and fat) were dissected from normal mice and incubated with the phage library obtained from the positive selection. After the incubation period, the mixture was centrifuged and the supernatant plated for titer and sequencing. Once individual sequences started to appear repetitively, these were resynthesized as peptides for affinity testing.

For the *in vivo* selection, the same phage library as for the *in vitro* selections was injected in the tail vein of mice followed by dissection of nerve tissue and isolation of phage. In each case isolated phage were reamplified and reinjected to iterate each selection step up to 8 times. Specifically, phage were injected into wild-type mice. Following a binding/washout period of 2–4 h, the mice were euthanized and nerve tissue (sciatic, brachial plexus, cranial nerves) were dissected, washed and homogenized. Homogenates were plated for titering and re-amplified for subsequent injections. Sample phage were sequenced after each round of selection. Once repeat sequences appeared, they were synthesized for affinity testing.

Peptide synthesis and fluorophore labeling. Peptides were either synthesized in our laboratory on an Agilent Prelude peptide synthesizer using standard protocols for fluorenylmethoxycarbonyl (Fmoc) solid-phase synthesis or made by AnaSpec. All peptides were acetylated at the N terminus and labeled on the C terminus by (either (Cy5-l-cysteinamide or ε-(fluorescein-5(6)-carbonyl)-L-lysinamide) (**Supplementary Fig. 3**). Carboxyfluorescein labeled peptides were generated by Fmoc synthesis with ε-(fluorescein-5(6)-carbonyl)-L-lysinamide. Cy5 labeling was done after cleavage from the synthesis resin by reacting the thiol group of the L-cysteinamide with Cy5 mono-maleimide (GE Healthcare). Peptides were purified to >95% purity using C-18 reversed phase high-performance liquid chromatography (HPLC) with a 20–50% acetonitrile gradient in 0.1% trifluoroacetic acid and confirmed by mass spectrometry.

Testing of nerve binding with fluorescently labeled peptides. Wild-type albino C57BL6 (Jackson Laboratory) or SKH1 (Charles River Laboratories) mice were treated intravenously with 150 nmoles of fluorescently labeled NP41 by tail vein injection. Following a 2–4 h wash-out period for FAM-NP41 or 5–6 h for Cy5-NP41, mice were anesthetized with ketamine and midazolam (80 mg/kg intraperitoneally), a skin incision was made over the dorsal surface of the hind legs and the sciatic nerves exposed bilaterally. Nerves were imaged using a Zeiss Lumar fluorescent dissecting microscope or a custom-made surgical fluorescence imaging system based on an Olympus dissecting microscope. Carboxyfluorescein and YFP were imaged with 450–490 nm excitation and 500–550 nm emission. Cy5 was imaged with 590–650 nm excitation and 663–738 nm emission.

Time course of nerve binding. Female 8-week-old SKH1 mice were anesthetized with ketamine and midazolam and a skin incision was made over the dorsal surface of the hind legs and the sciatic nerves exposed. A preinjection image was taken a dissecting microscope (Lumar Zeiss) and a monochrome CCD camera (Coolsnap). The mice were injected intravenously with 150 nmoles of FAM-NP41. Sequential fluorescence images were obtained as described above: 450–490 nm excitation and 500–550 nm emission, exposure 15 ms–5s. For quantification, integrated intensity was determined using ImageJ for nerve regions and compared to adjacent muscle or other nonnerve tissue. We analyzed 5–10 selected regions of 40 × 40 pixels of each type of tissue and all tissues were imaged using identical parameters. Background was subtracted using a measurement with identical settings in a region with no mouse and values were averaged.

Dose response of peptide binding. Female 8-week-old SKH1 mice (average weight 25 g) were treated with varying amounts of FAM-NP41 ranging from 15–5,000 nmoles. After a 2-h wash-out period, mice were euthanized and sciatic nerves exposed. Nerves and adjacent nonnerve tissue were delineated with Image J and relative fluorescence was measured. Quantification of fluorescence was then performed after subtraction of dark current and normalizing to uninjected specimens. For the mice injected with 5,000 nmoles of NP41, we found that background fluorescence was still very high at 2 h, making the contrast ratio low even though the absolute nerve fluorescence was very high. The skin incision on these mice was repaired and the mice allowed to awaken from anesthesia. At 6 h after initial NP41 administration, the mice were euthanized and the sciatic nerves exposed and analyzed as above.

Nerve labeling in tumor model. Syngeneic tumor grafts were generated in the laboratory with 8119 murine mammary adenocarcinoma cells[19]. We injected 1×10^6 cells intramuscularly into the left flank of albino C57BL/6 mice (Jackson Laboratory). Tumor isografts were monitored until tumor size was ~1 cm in largest diameter (~7–10 d). Cy5-ACPPD (2 nmoles)[19] and FAM-NP41 (150 nmoles) were administered through tail vein injection 48 and 2–3 h, respectively, in the same animal before imaging.

Toxicity and motor function. Female 8-week-old SKH1 mice (average weight 25 g) were treated with varying amounts of FAM- NP41 ranging from 15 to 5,000 nmoles. Generalized activity, behavior and weight gain were evaluated after single intravenous injection of 15–5,000 nmoles of FAM-NP41 on a daily basis for 3 d after injection. Thereafter, the mice were monitored three times per week for 8 weeks. We found that generalized activity, behavior and weight gain were similar between NP41-treated and control mice.

Nerve conduction studies. Maximal compound muscle action potential amplitude (CMAP) and nerve conduction latency were measured. Briefly, control female 8-week-old SKH1 mice and mice treated with FAM-NP41 were anesthetized with ketamine-midazolam and placed in a prone position. CMAP potentials were evoked (Grass stimulator) with stimulating electrode (Medtronics) placed 2 mm lateral to the midline. The recording electrode was an ear-clip electrode (Life-tech.com) placed on the digits of the hind foot and the reference electrode was placed on the heel of the foot. Maximal CMAPs were generated by gradually increasing the stimulation (5–10 V, 1 pulse per second, paired, 0.5–2 s duration) until a maximal, artifact-free tracing was obtained. The CMAP traces were captured on a digital oscilloscope (Tektronic). Nerve conduction latency was measured from the beginning of the stimulation to the start of the upslope. CMAP amplitude was measured from the start of the upslope to the peak. Data were analyzed using two-tailed Student's *t*-test.

Peptide metabolism. For liquid chromatography-mass spectrometry (LC-MS), each mouse urine sample was diluted and analyzed by reversed-phase HPLC with a 1 mm inner diameter, 15 cm length Higgins PLRP-S C18

column. The outlet from the HPLC (Michrom Magic with UV detector) was connected through a Jasco 920 fluorescence detector to the electrospray interface of a LTQ Orbitrap XL mass spectrometer. A 2 µl sample of mouse urine was diluted to 80 µl with solvent A, 0.1% formic acid in water. The HPLC had a 130 µl sample loop. The column temperature was 40 °C and the flow rate was 80 µl/min. After a 4 min delay (2% solvent B) for the injection, the gradient was 2 38% solvent B (0.1% formic acid in acetonitrile) in 37 min, followed by a 5 min step of 90% B. The pure peptide diluted from stock solution eluted at ~24 min. UV absorbance (single wavelength, 215 nm), fluorescence and mass spectral chromatograms were collected simultaneously for each LC-MS run. FAM and Cy5 fluorescences were measured at excitation/emission wavelength settings of 480/510 and 640/680 nm respectively. The fluorescence detector flow cell volume was 5 µl. The Orbitrap was set for 5 s scans with 30,000 resolution from 100 to 1,800 *m*/*z*. The entire HPLC output went into the mass spectrometer without splitting.

Effect of nerve injury on labeling. Wild-type mice were anesthetized and the left sciatic nerve exposed and crushed with microforceps for 3–5 s. Muscular contractions during the crush and immediately afterwards were monitored to ensure uniformity of the injury. The skin incision was then closed and mice returned to their cages to recover. At varying times after crush injury, FAM-NP41 (150 nmoles) was administered intravenously. After wash-out for 2–3 h, mice were anesthetized, bilateral sciatic nerves exposed and fluorescent images obtained. Nerve and adjacent muscle fluorescence were measured using ImageJ software by measuring standardized boxed regions. Crushed and contralateral control nerve fluorescence were compared for each animal.

Human nerve labeling. Recurrent laryngeal nerves and adjacent muscle obtained from patients undergoing total laryngectomy for laryngeal cancer at the time of surgery were incubated with FAM-NP41 at 50 µM for 15 min and washed three times in saline for 15 min each. The nerve and muscle segments were then placed on a black nonfluorescent plate and imaged (Maestro, CRI). The nerve segments were then embedded in Tissue-Tek, frozen and cryosectioned. We then imaged 7–10 µm cryosections with standard fluorescence microscopy. Adjacent sections were stained with hematoxylin and eosin (H&E) and imaged by transmitted light.

doi:10.1038/nbt.1764